Journal of Biomolecular NMR, 2 (1992) 19–32
ESCOM

J-Bio NMR 041

Conformation of 6,7-dimethyl-8-ribityllumazine bound to β-subunits of heavy riboflavin synthase: Transferred nuclear Overhauser effect (TrNOE) studies employing ω_1-^{13}C-filtered NOESY including a novel technique for zero quantum suppression

Hartmut Oschkinat[a,*], Karin Schott[b] and Adelbert Bacher[b]

[a]*Max-Planck-Institut für Biochemie, D-8033 Martinsried, Germany*
[b]*Technische Universität München, Lehrstuhl für Organische Chemie und Biochemie, D-8046 Garching, Germany*

Received 29 April 1991
Accepted 12 August 1991

Keywords: Heavy riboflavin synthase; Lumazine; Transferred nuclear Overhauser effect; Dynamical NOE

SUMMARY

The β-subunits of heavy riboflavin synthase catalyze the formation of 6,7-dimethyl-8-ribityllumazine. The interaction of the ^{13}C-labelled enzyme product with isolated β-subunits was studied by transfer NOE measurements using ω_1-^{13}C-filtered NOESY and ^{13}C-^{1}H-relayed NOESY. The advantages of these techniques are the removal of residual enzyme signals, the simplification of zero quantum suppression, and the improvement of water suppression which enabled the semiquantitative study of ^{1}H-^{1}H distances of the ligand in the bound state. The preferred conformation of the ribityl side chain was calculated on the basis of the measured distances.

INTRODUCTION

The lumazine synthase/riboflavin synthase complex (heavy riboflavin synthase) of *Bacillus subtilis* catalyzes the terminal reactions in the biosynthesis of riboflavin which is shown in Scheme 1 (Bacher et al., 1980a; Volk and Bacher, 1990). More specifically, the β-subunits of the enzyme catalyze the condensation of L-3,4-dihydroxy-2-butanone 4-phosphate (Scheme 1, (**1**)) with 5-amino-6-ribitylamino-2,4(1H,3H)-pyrimidinedione (**2**) in a reaction yielding 6,7-dimethyl-8-ribityllumazine (**3**) and phosphate (Neuberger and Bacher, 1986; Volk and Bacher, 1988, 1990). The

* To whom correspondence should be addressed at EMBL, Meyerhofstr. 1, D-6900 Heidelberg, Germany.

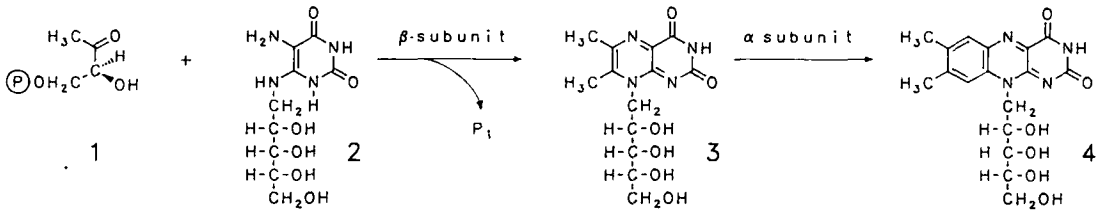

Scheme 1.

subsequent dismutation of the lumazine (**3**) which is catalyzed by the α-subunits yields riboflavin (**4**) and **2** (see also Scheme 2).

The enzyme has a highly unusual structure. Sixty β-subunits form an icosahedral capsid in which three α-subunits are enclosed (Bacher et al., 1980a,b, 1986). The structure of the capsid has been investigated by X-ray crystallography at a resolution of 3.3 Å (Ladenstein et al., 1987, 1988). Subsequent to the dissociation of the native enzyme under mild conditions, the β-subunits reassociate forming large aggregates with the shape of hollow spheres with diameters around 280 Å (Bacher et al., 1986). The β-subunit aggregates are catalytically active, albeit at a substantially lower rate than the native enzyme (Neuberger and Bacher, 1986). The system with the isolated β-units was chosen for the current experiments, since 6,7-dimethyl-8-ribityllumazine is a substrate for the α-subunit and would therefore be rapidly decomposed by the native enzyme.

In this investigation, we have applied the so-called Dynamical or Transfer NOE experiment (TrNOE) (Albrand et al., 1979; Hyde et al., 1980; Clore and Gronenborn, 1983; Landy and Rao, 1989) to derive the conformation of the lumazine bound to the protein. Three conditions should be fulfilled to enable a successful study: (i) The positive NOE of the free ligand has to be suppressed, (ii) the effects of 'spin diffusion' have to be minimized, and (iii) it must be possible to identify signals originating from protein–protein interactions or to avoid contributions of such signals to the intra-ligand NOEs. In order to fulfill the first and second requirements, NOESY experiments with short mixing times have to be applied. ^{13}C-labelled lumazine derivatives were used to fulfill the third condition, enabling H,C-relayed-H,H-NOESY- and ω_1-X-filtered NOESY experi-

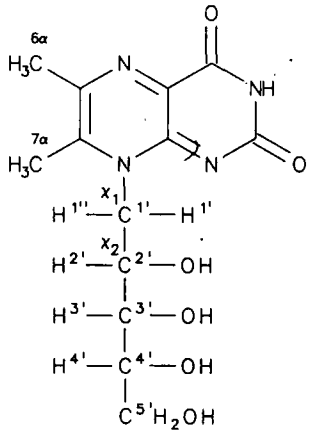

Scheme 2.

ments (Otting et al., 1986; Senn et al., 1987). The latter effect could not be obtained by increasing the concentration of the ligand as this would require recording of NOESY spectra with longer mixing times leading to an interference of the positive NOE from the free ligand with the negative one of the bound ligand.

Isotope labelling and the use of ω_1-filtered NOESY also offers the possibility of minimizing zero quantum contributions in NOESY spectra at short mixing times using a new method. This was an important side effect of the labelling, because some of the NOESY cross peaks showed significant contributions of zero quantum signals.

MATERIALS AND METHODS

Materials

The preparation of (1'-R)-[1'-^{2}H]6,7-dimethyl-8-ribityllumazine and [6α,7α-$^{13}C_1$]6,7-dimethyl-8-ribityllumazine has been described elsewhere (Sedlmaier et al., 1987; Keller et al., 1988). [1'-^{13}C]- and [2'-^{13}C]6,7-Dimethyl-8-ribityllumazine were prepared from [1-^{13}C]- and [2-^{13}C]ribose (Omicron Inc., South Bend, IN) via 5-nitro-6-ribitylamino-2,4(1H,3H)-pyrimidinedione as intermediate (Bacher, 1986; Nielsen et al., 1986). β-Subunits of heavy riboflavin synthase from *B. subtilis* were prepared as described elsewhere (Schott et al., 1990).

NMR measurements

(a) Samples

Three differently ^{13}C-labelled lumazines and the unlabelled ligand were used for the measurements, the labels being in the 1', 2', and (6α,7α) positions. All distances used for the structure calculations were taken from spectra of the labelled derivatives. The characteristics of the different samples used are shown in Table 1.

(b) Pulse sequences

Five different pulse sequences were used to study the TrNOE effect: a normal NOESY sequence to record spectra from the sample with the unlabelled compound (Fig. 1a), ω_1-^{13}C-filtered NOESY sequences (Figs. 1b, c and d) and a H,C-relayed-H,H-NOESY (Fig. 1e). The sequences used

TABLE 1
SAMPLES AND PULSE SEQUENCES USED

No.	^{13}C-label	[c]Ligand (mM)	[c]Enzyme (mM)	Solvent[a]	pH[b]
I	Unlabelled	9.5	0.7	D_2O	7.0
II	[1'-^{13}C]	18.3	1.5	D_2O	6.0
III	[2'-^{13}C]	20.8	1.7	D_2O	6.0
IV	[6α,7α-$^{13}C_1$]	20.8	1.7	97%H_2O/3%D_2O	6.0

[a]Using 100 mM phosphate buffer.
[b]Uncorrected glass electrode reading.

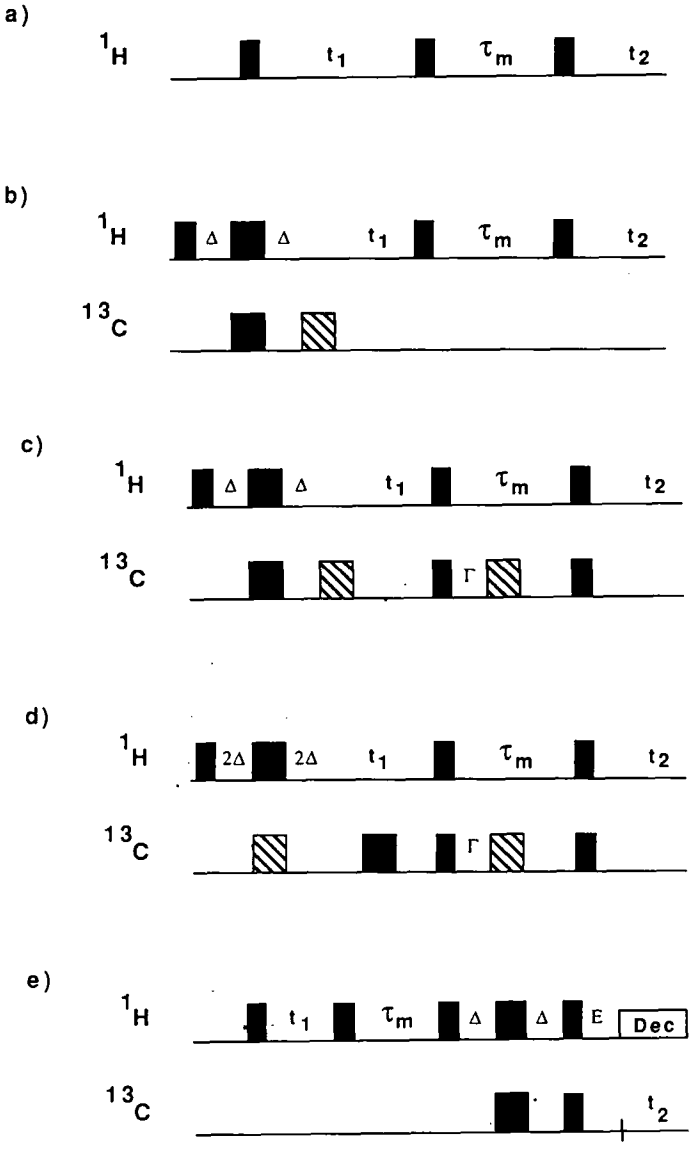

Fig. 1. NMR pulse sequences used: normal NOESY (a); ω_1-X-filtered NOESY (b,c,d) and heteronuclear relayed-H,H-NOESY (e). The delay Δ for evolution of the heteronuclear couplings is $(4J)^{-1}$. For the choice of Γ, see text. The phase cycling of the normal NOESY sequence (a) was: x, $-$x for the first pulse, x for the second, and 2(x), 2(y), 2($-$x), 2($-$y) for the third pulse. The phase of the receiver was (x, $-$x, $-$x, x, y, $-$y, $-$y, y). To achieve the filtering effect, a period for the evolution of the heteronuclear couplings followed by a 180° pulse (hatched drawing) is inserted into the sequence as shown in (b). Each phase increment of the phase cycle above is executed twice with and without the application of the editing pulse, and the receiver phase is inverted for the experiments with the editing pulse, hence the number of scans is doubled. The same procedure is applied involving the hatched pulse in the mixing time of sequence c to eliminate zero quanta. The 90° pulses applied to the carbon are used with the same phase settings as the corresponding pulses applied to the protons. The phase cycling of all 180° refocussing pulses (x, $-$x) is performed with lowest priority.

The phase cycling of sequence (e) is simply the combination of a NOESY and an INEPT phase cycle. E was chosen appropriately for optimum refocusing of the CH_3-carbon multiplet lines.

to record the ω_1-X-filtered NOESY shown in Figs. 1b and c are different with respect to the mixing pulses applied to the carbon, and the sequence in Fig. 1d yields ω_1-decoupled spectra. Decoupling in ω_2 was not applied as it was neither useful nor necessary in this study.

The main characteristics of the spectra obtained with the pulse sequence 1b are the disappearance of the strong parallel transitions in the diagonal multiplets. It was preferable to record spectra of the 1'-labelled lumazine without decoupling in F_2, as in this way the best separation of the expected cross peaks between the protons at C1' from the H_2O signal was obtained. The spectrum can be understood as consisting of the superposition of two different molecules, i.e. one molecule seeing the carbon spin with α-polarisation, the other molecule in the β-state. The interpretation of the spectrum in the simple manner applied to normal NOESY spectra is allowed when only resonances with the same carbon polarisation are compared, i.e. when only cross peaks with the same frequency in ω_1 are compared. This may be calculated with the usual procedures (Oschkinat and Bermel, 1989). If cross peaks which involve a flip of the carbon are considered, a more detailed interpretation (Oschkinat et al., 1989) is necessary.

The special advantage of the sequence in Fig. 1c and of its ω_1-decoupled version (Fig. 1d) lies in the opportunity to achieve efficient suppression of proton zero quantum coherences (Rance et al., 1985) by only doubling the number of scans. The zero quantum coherences which disturb the spectrum most are described by four terms of the type $I_{y,x}{}^{H1}I_{x,y}{}^{H2}$, considering a three-spin system with the spins H1, H2, and C. Within a period $(2J_{CH1}+2J_{CH2})^{-1}$ they evolve to terms like $I_{x,y}{}^{H1}I_{y,x}{}^{H2}I_z{}^{C}$ whose sign can be inverted by a π-pulse applied to the carbon at that time. They can be eliminated by subtracting two experiments with or without π-pulse. A problem occurs insofar as only certain types of zero quantum signals will be suppressed completely due to the dependency on the sum of the couplings, which may be strongly different in individual cases. For example, if H1 and H2 are both attached to the labelled carbon, the delay Γ has to be very short (i.e. 500^{-1} s). However, the fact that only certain zero quantum coherences are suppressed does not matter in our case, as selectively labelled compounds are investigated.

The pulse sequence for the X-relayed H,H-NOESY (see Fig. 1e) is particularly simple: A normal NOESY sequence is followed by an INEPT experiment to transfer the magnetization to the carbon. Since in our case only a one- or two-line carbon spectrum is observed, the refocusing pulses after the magnetization transfer were omitted. The resulting spectrum consists of the carbon spectrum in ω_2 and a 1D-transient NOE spectrum in ω_1, with the proton attached to this carbon appearing as the one which was inverted.

Semiquantitative evaluation of TrNOE experiments

Dissociation equilibria of enzyme–substrate complexes are usually assumed to be second-order reactions in the formation of the complex and first-order in the dissociation of the complex:

$$E+L \underset{k_{off}}{\overset{k_{on}}{\rightleftarrows}} EL \qquad (1)$$

In TrNOE studies, it is the equilibrium of free ligand and complex which is monitored. Notably, only systems which show simple equilibria may lead to sensible results. Substantial cross peaks be-

tween enzyme protons and substrate protons are not expected with the rate constants and concentrations involved, although some exceptions are known (Bothner-By and Gassend, 1973).

With recourse to the initial rate approximation, the effect of this equilibrium on the amplitude A_{ij} of a cross peak in the NOESY spectrum of the enzyme–substrate system is given by (Jeener et al., 1979; Kumar et al., 1980; Landy and Rao, 1989):

$$A_{ij}(M_Z^A + M_Z^a \rightarrow M_Z^X + M_Z^x) = \rho_b \sigma_{ax} + \rho_F \sigma_{AX} \tag{2}$$

where small indices indicate the bound form and the capital ones the free form. The observed intensity of the cross peak between two signals displays σ_{ax} and σ_{AX}, both weighted with the molar fractions of the respective species, if very short mixing times are applied. Utilizing the approximation given above, the distances within the ligand molecule can be determined provided a reference distance is given.

Molecular dynamics calculation

NOE-restrained molecular dynamics were performed using the software package DISCOVER (Biosym Inc.) (Hagler, 1979).

The NOE potential used was of a skewed biharmonic form:

$$E\,noe(r) = \begin{cases} c_1(2r - r_1 - r_{1max})\ (r_{1max} - r_1) & r < r_{1max} \\ c_1(r - r_1)^2 & r_{1max} < r < r_1 \\ 0 & r_1 < r < r_2 \\ c_2(r - r_2)^2 & r_2 < r < r_{2max} \\ c_2(2r - r_2 - r_{2max})\ (r_{2max} - r_2) & r_{2max} < r \end{cases}$$

in which r is the calculated interatomic distance, r_1 and r_2 are the target pushing and pulling distances, and $r_{1,2max}$ are given by

$$r_{1max} = r_1 - force1_{max}/2c_1 \qquad r_{2max} = r_2 + force2_{max}/2c_2$$

containing the force constants c_1 and c_2 which are temperature.dependent. They are defined as

$$c_1 = RTS/2(\Delta_+)^2 \qquad c_2 = RTS/2(\Delta_-)^2$$

where R is the gas constant, T is the absolute temperature, S is a scale factor and Δ_+ and Δ_- are the pulling and pushing error estimates, respectively.

A set of 36 structures with systematic variation of the dihedral angles between H1′ and H2′ (χ_1) and between H2′ and H3′ (χ_2), respectively, was used to generate starting structures by forced dynamics at 300 K followed by forced minimization. These starting structures were used in NOE-constrained dynamics simulations at 700 K for 8 ps during which the scale factor S was gradually raised to a final level of 4.0. After cooling, dynamics simulation was continued at 300 K with a scale factor of 1 for 1 ps which was followed by energy minimization. The target pushing and pulling distances were kept to the same value ($r_1 = r_2$), the constants force 1_{max} and force 2_{max} which

TABLE 2
INTERATOMIC DISTANCES OBTAINED FROM NMR MEASUREMENTS AND MOLECULAR DYNAMICS SIMULATIONS

Interaction	Distances (Å) ($r_1 = r_2$)	Error limits (Å)	Average distances and their standard deviations in the 32 structures shown in Fig. 5	
			Before minimization	After minimization
7α-CH_3-H1′	3.2	∞ /−0.4	4.1±0.2	4.1±0.1
7α-CH_3-H1″	2.7	+0.4/−0.4	2.9±0.2	2.7±0.1
H1″-H2′	3.0	+0.3/−0.3	3.1±0.1	3.1±0.1
H1′-H2′	2.6	+0.3/−0.3	2.7±0.2	2.6±0.1
H1″-H4′	3.5	∞ /−0.3	3.7±0.4	3.5±0.1
H1′-H4′	2.6	+0.3/−0.3	2.6±0.3	2.4±0.1
H2′-H3′	2.5	+0.3/−0.3	2.5±0.1	2.5±0.1
H1′-H3′	3.4	∞ /−0.3	3.9±0.2	3.8±0.1
H1″-H3′	3.4	∞ /−0.3	3.9±0.1	3.9±0.1
H2′-H4′	3.0	+0.3/−0.3	3.1±0.2	3.1±0.1

determine the cutoff were chosen to 100 kcal/mol/Å^2. The error limits for all distances measured with a mixing time of 20 ms were chosen to 0.3 Å, the estimates of the distances involving the 7α-methyl group and the protons at C1′ were supplemented by error limits of 0.4 Å. The individual target distances together with the error limits are shown in Table 2. The choice of like pushing and pulling target distances in conjunction with small error limits of 0.3 Å for distances within the ribityl chain seems justified by the good S/N ratio of the ω_1-filtered NOESY spectra and the short mixing times used. The effective force constants applied were 30.85 kcal/mol^{-1}Å^{-2} at 700 K with a scaling factor of 4 and an error estimate of 0.3, whereas the corresponding value at 300 K and a scaling factor of 1 is 3.3 kcal/mol^{-1}Å^{-2}.

RESULTS

Distance determination

TrNOE studies depend on the possibility of acquiring data in an appropriate 'time window' for accurate distance evaluation. This means that a suitable compromise between substrate/enzyme concentrations and mixing time – depending on the binding constant – has to be chosen, in order to determine distances in a sufficiently accurate manner. In the case of ligands with positive NOE the molar fractions of bound and free ligand must be adjusted adequately to emphasize the strong negative NOE arising from the bound state. In other words, the term (ρ_b σ_{ax}) must dominate the relevant relaxation matrix elements (right side of Eq. 2). Consequently, only a 10-fold excess concentration of the ligand compared to the concentration of the monomeric form of the enzyme was used. Also, comparatively short mixing times (20 and 40 ms) were used for the NOESY spectra in order to monitor the build up of the NOEs in the linear range. As a result, the enzyme signals were still visible in the NOESY spectra. They may interfere with the intra-ligand cross peaks and hence lead to corrupt integrals. This problem was solved by the utilization of the ^{13}C-labelled lumazines which permitted various ω_1-X-filtered NOESY experiments (Figs. 1b–d) and a heteronuclear re-

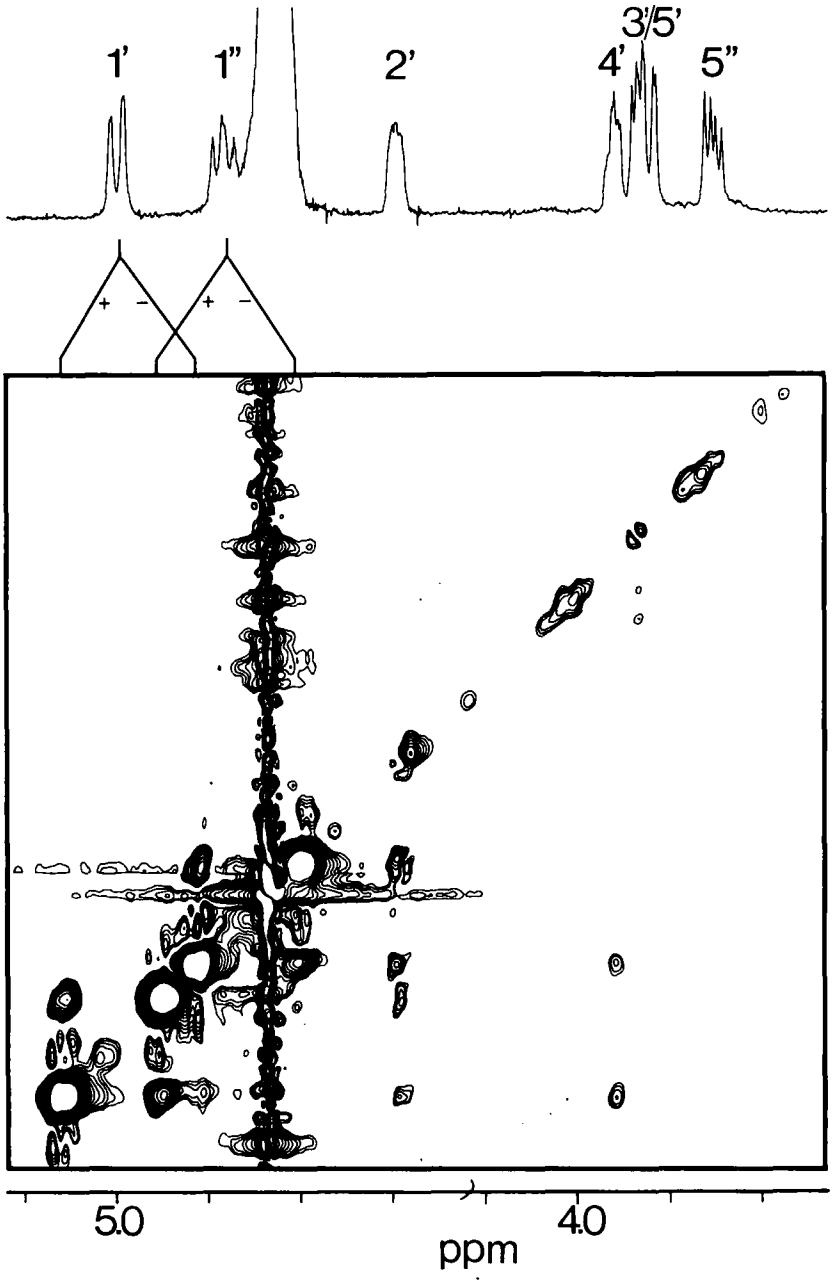

Fig. 2. Part of the ω_1-^{13}C-filtered NOESY without carbon mixing pulses (Fig. 1b) of sample II (C1'-labelled, 100% D_2O) recorded with a mixing time of 20 ms. The 1D spectrum of the unlabelled ligand without protein is shown on top. As a consequence of the editing process, the protons bound to the labelled carbon appear as doublets in ω_1, both components in anti-phase with respect to each other. This is indicated below the 1D spectrum, together with the sign of the components. The cross-peak pattern observed proves that the effects due to migration of magnetization through several pathways is not severe, e.g. no cross peaks are observed between H1' and H3', but rather strong ones between H1' and H4'. The absence of carbon mixing pulses allows only small cross peaks to appear in the positions of the parallel transitions; therefore it is possible to integrate the amplitude of the neighbouring signals due to geminal NOEs with greater certainty.

layed-H,H-NOESY (Fig. 1e). The distances were determined assuming a uniform correlation time for the interproton vectors. This also contains the assumption that all atoms of the sugar chain are in contact with the enzyme, which is justified by the results obtained by X-ray analysis of similar systems (Ladenstein et al., 1987, 1988). Furthermore, this allows the conclusion that the amount of spin diffusion observed within the ligand must be of the same order as between ligand and protein.

The distances involving the protons at C1′ and other sugar protons were taken from spectra recorded with the pulse sequences in Figs. 1b and c using the 1′-labelled lumazine. The integration of the cross peaks between the H1′ and the H2′ and H4′ protons, respectively, in the ω_1-X-filtered NOESY spectrum of Fig. 2 yielded distances of 2.6 Å in both cases. The NOE between the two protons at C1′ was taken as a reference. The sequence in Fig. 1b was used to record this spectrum in order to avoid the strong parallel transitions around the diagonal, which would hamper accurate integration of the reference NOE. The absence of a strong cross peak between H1′ and H3′ indicated a long distance between these two protons. The relative short distance between the H1′ and H4′ protons is not due to the migration of magnetization via other pathways, as no cross peak involving the 3′ proton occurs. This also proves that the lifetime of the bound state is short enough to allow the application of the initial rate approximation in general. The distance of 2.6 Å between H1′ and H2′ indicates a perfect cis conformation. A problem occurred insofar as the

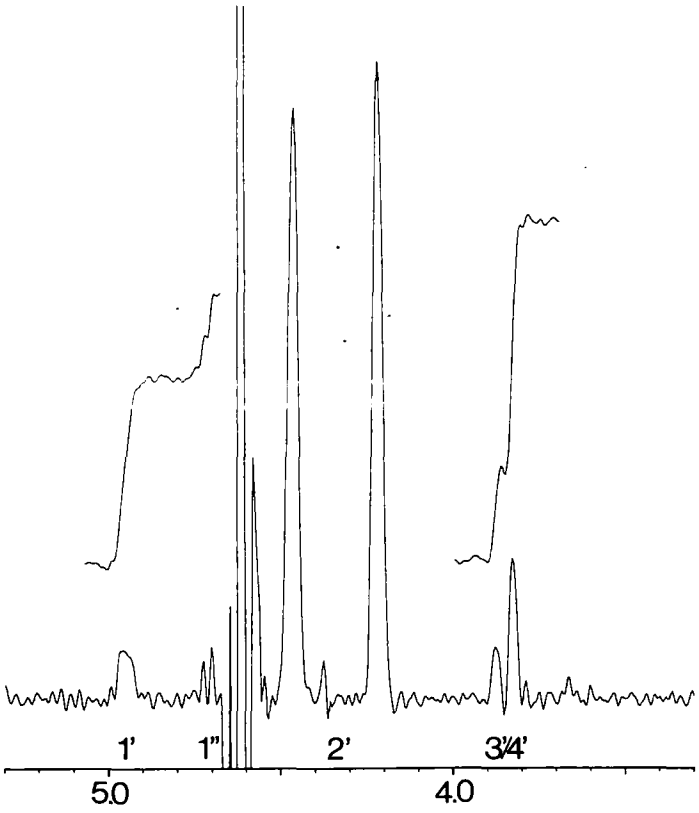

Fig. 3. Cross section along F_2 through the maximum of the only occurring F_1-signal in the ω_1-filtered NOESY of the 2′-labelled derivative (sample III, 100% D_2O). The integrals are given to indicate the relative size of the cross peaks.

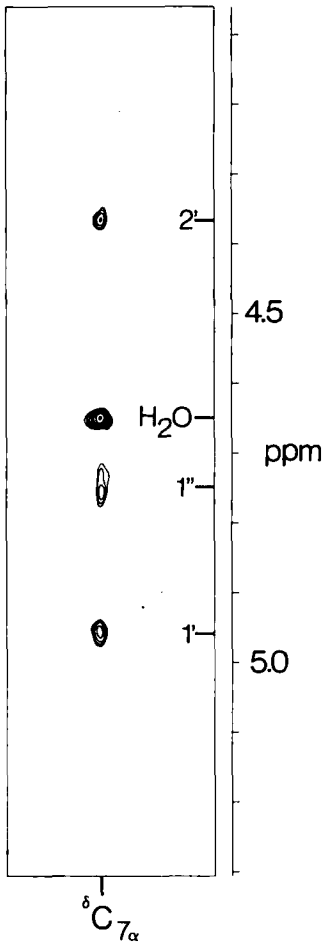

Fig. 4. The relevant part of the C-relayed-H,H-NOESY of sample IV (6α,7α-labelled, 97% H_2O) recorded with a mixing time of 40 ms showing the NOE between the carbon resonance of the 7α-methyl group and the sugar protons. The amplitude of the two cross peaks between the methyl protons and the protons at C1′ are also distinctly different in the spectrum recorded with 20 ms.

cross peak between H1″ and H2′ was contaminated by zero quantum coherences. Therefore, a spectrum with the sequence in Fig. 1c, optimized for the suppression of the relevant zero quantum coherences, was recorded. This also showed that the cross peak between H1″ and H2′ is of smaller amplitude than the one between H1′ and H2′. The integrals correspond to 2.6 Å and 3.0 Å. The latter is expected for a trans arrangement.

An independent control is given by the ω_1-filtered NOESY spectrum of the 2′-labelled derivative. The section through the maximum of the 2′ signal along F_2 is shown in Fig. 3. The integrals display the cis/trans arrangement to H1′ and H1″ as well as the short distance between H2′ and H3′. Values for the distances between H2′ and H3′/H4′ of 2.5 Å and 3.0 Å, respectively, were obtained by utilizing the distances between the protons at C1′ and C2′ as references.

A problem occurred in the evaluation of the distances between the 7α-CH_3 group and the two

protons at C1′. As it was only possible to measure this interaction with a ^{13}C-relayed-H,H-NOESY experiment, no useful reference was given and it was only possible to distinguish the length of both distances in a qualitative manner. Two spectra with different mixing times (20 and 40 ms) were recorded. The spectra consisted of two carbon lines in ω_2 originating from the two methyl groups, of which the one at 21.2 ppm showed cross peaks to the protons at C1′ and C2′ as well as to the H_2O resonance. The relevant part of the spectrum with a mixing time of 40 ms is shown in Fig. 4, and reveals some spin diffusion. The spectrum recorded with the shorter mixing time also showed a stronger signal to the H1″ proton, but its signal-to-noise ratio was not good enough for proper integration of the cross peaks. The actual values for the distances were determined on the graphics system by rotating the ribose side chain around the bond to the ring. The closest distance between the methyl group and H2″ which avoids a staggered conformation is 2.7 Å. For the other distance, a lower limit of 3.2 Å was observed to be appropriate.

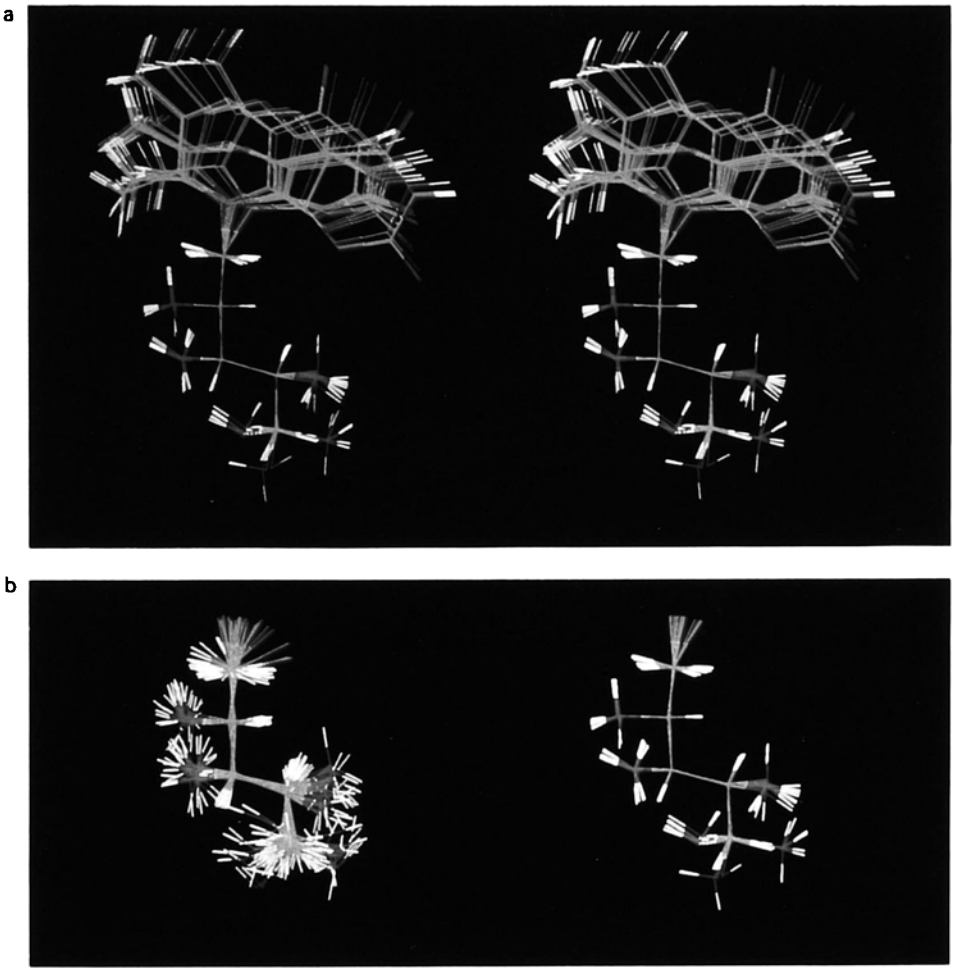

Fig. 5. (a) Structure of the ligand calculated from the NOE data in Table 1 (stereo pair). (b) Structure of the ribityl chain before (right) and after (left) minimization.

Structure calculation

The set of 6 measured distances was supplemented by 4 non-NOEs, which were used as additional constraints on the basis of negligible amplitudes of the relevant cross peaks. Due to the graphical inspection of the possible conformations around χ_1, a minimum value of 3.2 Å for the distance between the 7α-CH_3 group and H1′ was chosen. Minimum distances of 3.5 Å between H1″ and H4′ and of 3.4 Å for the interaction of the protons at C1′ with H3′, respectively, were chosen because of negligible cross peaks. The distances as subjected to the calculations are summarized in Table 2. The calculation yielded 32 very similar structures (out of 36 calculations) with well-determined conformations around χ_1 and χ_2. This is also shown in Table 2 separately for the structures obtained before minimization and for those obtained after minimization. The superposition of these 32 structures is shown in Fig. 5a, the ribityl chains before and after minimization are compared in Fig. 5b. The bad definition of the end of the ribityl chain is due to the lack of data (H3′ and H5′ are too close to each other to allow a quantitative evaluation of NOE involving H4′). Figure 5a suggests that the rotations of the 7α/6α-methyl groups were fixed during the calculations. This is in fact a result of the minimization, which is sensitive to the sterical hindrance of the two neighbouring methyl groups. The four structures which are not given showed either deviations at the end of the ribityl chain, which is expected because of the lack of restraints, or different conformations due to a variation of the angle χ_2.

DISCUSSION

Isotope filtering offers several advantages for the study of enzyme–ligand interactions by NMR. Most important, subtraction of the enzyme signals allows the integration of the cross peaks in NOESY spectra recorded at short mixing times. An additional advantage is the improved suppression of the residual water resonance and of most of the T_1-noise. The ω_1-X-filtered NOESY experiment may be used in different manners, with or without mixing pulses at the carbon frequency. Using mixing pulses for protons only has the advantage that no strong cross peaks due to parallel transitions along the diagonal occur, enabling in our case the integration of important cross peaks. However, if mixing pulses are applied to the hetero-nucleus, contributions to the spectrum due to zero quantum coherences can be suppressed by a subtraction procedure. This technique is important in the context of TrNOE studies, because such signals are expected to be large, despite a considerable broadening of the ligand signals.

The calculation of the preferred conformation of the lumazine bound to the β-subunit aggregates shows a bend in the ribityl side chain which leads to a rather short distance between the H1″ proton and the H4′ proton. The calculations showed that the measured values are well in agreement with an energetically favoured conformation.

It has been shown that 6,7-dimethyl-8-ribityllumazine can form anions with an unusual structure by covalent hydration involving the 2′- or 3′-hydroxy group of the ribityl side chain. This leads to structures with additional 5- or 6-membered rings which have been studied in some detail by NMR spectroscopy (Beach and Plaut, 1970, 1971; Pfleiderer et al., 1971; Bown et al., 1986). 6,7-Dimethyl-8-ribityllumazine is converted to riboflavin by the α-subunits of riboflavin synthase, and it has been proposed by Plaut and Beach that the mechanism of this enzyme-catalyzed reaction could proceed via the covalently hydrated state of the substrate (Plaut and Beach, 1975, 1976).

The present study deals with the β-subunits of riboflavin synthase for which 6,7-dimethyl-8-ribityllumazine is the product and not the substrate of the enzyme-catalyzed reaction. It is obvious from the data that the product is bound to this protein in the open chain form as opposed to one of the possible covalent hydrate structures.

It should be noted that the experiments were performed with an artifactual, albeit catalytically active, aggregate of β-subunits.

ACKNOWLEDGEMENTS

This work was supported by Grant No. 321/4003/0318909A from the Bundesministerium für Forschung und Technologie, by the Deutsche Forschungsgemeinschaft and by the Fonds der Chemischen Industrie. We are indebted to Dr. Milton Stubbs for streamlining the English. Skillful technical assistance of Angelika Kohnle and Astrid König is acknowledged. We also thank Dr. J. Brandt and F. Wendling for help with structure calculations.

REFERENCES

Albrand, J.P., Birdsall, B., Feeney, J., Roberts, G.C.K. and Burgen, A.S.V. (1979) *Int. J. Biol. Macromol.*, **1**, 37–41.

Bacher, A. (1986) *Methods Enzymol.*, **122**, 192–199.

Bacher, A., Baur, R., Eggers, U., Harders, H., Otto, M.K. and Schnepple, H. (1980a) *J. Biol. Chem.*, **255**, 632–637.

Bacher, A., Mailänder, B., Otto, M.K., Schnepple, H. and Ben-Shaul, Y. (1980b) In *Flavins and Flavoproteins* (Eds, Yagi, K. and Yamano, T.) Japan Scientific Societies Press, Tokyo, pp. 579–586.

Bacher, A., Ludwig, H.C., Schnepple, H. and Ben-Shaul, Y. (1986) *J. Mol. Biol.*, **187**, 75–86.

Beach, R.L. and Plaut, G.W.E. (1970) *Biochemistry*, **9**, 760–770.

Beach, R.L. and Plaut, G.W.E. (1971) *J. Org. Chem.*, **36**, 3937–3943.

Bothner-By, A.A. and Gassend, R. (1973) *Ann. N.Y. Acad. Sci.*, **222**, 668–676.

Bown, D.H., Keller, P.J., Floss, H.G., Sedlmaier, H. and Bacher, A. (1986) *J. Org. Chem.*, **51**, 2461–2467.

Clore, G.M. and Gronenborn, A.M. (1983) *J. Magn. Reson.*, **53**, 423–442.

Hagler, A.T. (1979) *J. Am. Chem. Soc.*, **101**, 5122–5130.

Hyde, E.I., Birdsall, B., Roberts, G.C.K., Feeney, J. and Burgen, A.S.V. (1980) *Biochemistry*, **19**, 3738–3746.

Jeener, J., Meier, B.H., Bachmann, P. and Ernst, R.R. (1979) *J. Chem. Phys.*, **71**, 4546–4553.

Keller, P.J., Le Van, Q., Kim, S.-U., Bown, D.H., Chen, H.-C., Kohnle, A., Bacher, A. and Floss, H.G. (1988) *Biochemistry*, **27**, 1117–1120.

Kumar, A., Ernst, R.R. and Wüthrich, K. (1980) *Biochem. Biophys. Res. Commun.*, **95**, 1–6.

Ladenstein, R., Bacher, A. and Huber, R. (1987) *J. Mol. Biol.*, **195**, 751–753.

Ladenstein, R., Schneider, M., Huber, R., Bartunik, H.-D., Wilson, K., Schott, K. and Bacher, A. (1988) *J. Mol. Biol.*, **203**, 1045–1070.

Landy, S.B. and Rao, B.D.N. (1989) *J. Magn. Reson.*, **81**, 370–377.

Neuberger, G. and Bacher, A. (1986) *Biochem. Biophys. Res. Commun.*, **139**, 1111–1116.

Nielsen, P., Neuberger, G., Fujii, I., Bown, D.H., Keller, P.J., Floss, H.G. and Bacher, A. (1986) *J. Biol. Chem.*, **261**, 3661–3669.

Oschkinat, H. and Bermel, W. (1989) *J. Magn. Reson.*, **81**, 220–225.

Oschkinat, H., Limat, D., Emsley, L. and Bodenhausen, G.J. (1989) *J. Magn. Reson.*, **81**, 13–42.

Otting, G., Senn, H., Wagner, G. and Wüthrich, K. (1986) *J. Magn. Reson.*, **70**, 500–505.

Pfleiderer, W., Mengel, R. and Hemmerich, P. (1971) *Chem. Ber.*, **104**, 2273–2292.

Plaut, G.W.E. and Beach, R.L. (1975) In *Chemistry and Biology of Pteridines* (Ed, Pfleiderer, W.) Walter de Gruyter, Berlin, New York, pp. 101–124.

Plaut, G.W.E. and Beach, R.L. (1976) In *Flavins and Flavoproteins* (Ed, Singer, T.P.) Elsevier, Amsterdam, pp. 737–746.

Rance, M., Bodenhausen, G., Wagner, G., Wüthrich, K. and Ernst, R.R. (1985) *J. Magn. Reson.*, **62**, 497–510.

Schott, K., Ladenstein, R., König, A. and Bacher, A. (1990) *J. Biol. Chem.*, **265**, 12686–12689.
Sedlmaier, H., Müller, F., Keller, P.J. and Bacher, A. (1987) *Z. Naturforsch.*, **420**, 425–429.
Senn, H., Otting, G. and Wüthrich, K. (1987) *J. Am. Chem. Soc.*, **109**, 1090–1092.
Volk, R. and Bacher, A. (1988) *J. Am. Chem. Soc.*, **110**, 3651–3653.
Volk, R. and Bacher, A. (1990) *J. Biol. Chem.*, **265**, 19479–19485.